Cell Reports Medicine, Volume *2*

Supplemental information

NOTCH3-targeted antibody drug conjugates regress tumors by inducing apoptosis in receptor cells and through transendocytosis into ligand cells

Kenneth G. Geles, Yijie Gao, Andreas Giannakou, Latha Sridharan, Ting-Ting Yamin, Jing Zhang, Riyez Karim, Joel Bard, Nicole Piche-Nicholas, Manoj Charati, Andreas Maderna, Judy Lucas, Jonathon Golas, Magali Guffroy, Steven Pirie-Shepherd, Marc Roy, Jessie Qian, Tania Franks, Wenyan Zhong, Christopher J. O'Donnell, Lioudmila Tchistiakova, Hans-Peter Gerber, and Puja Sapra

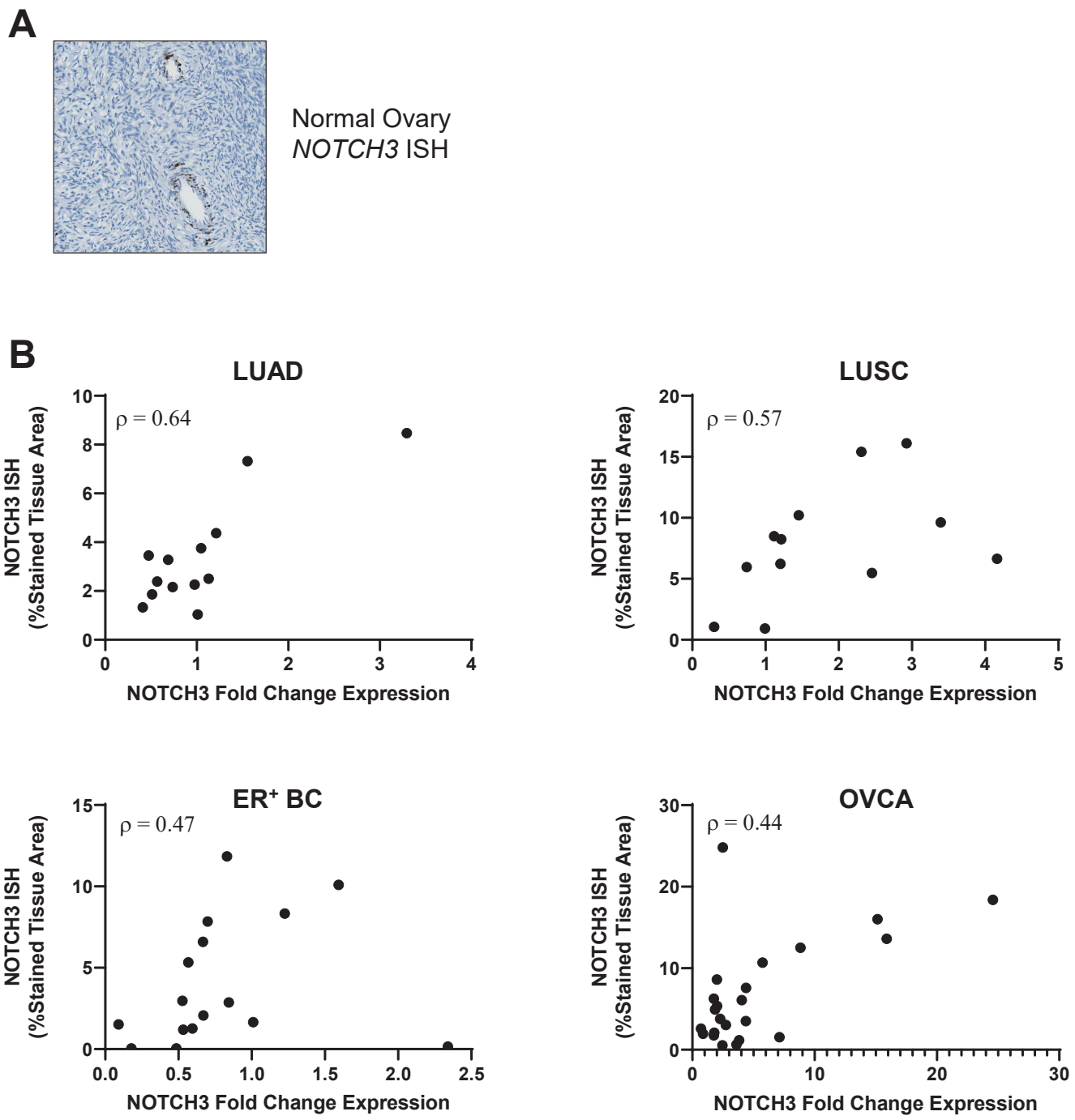

Figure S1. *NOTCH3* is Overexpressed in Multiple Human Tumors. Related to Figure 1.

(A) *NOTCH3* ISH staining in a normal ovarian tissue section. (B) Spearman's correlation plots of primary human tumor *NOTCH3* ISH quantitation versus qRT-PCR data. Correlation of the ISH and qRT-PCR data shows positive correlation between these two endpoints for each tumor set evaluated. Additionally, the qRT-PCR data and digital image analysis of *NOTCH3* ISH staining on sections of each tumor report a range of *NOTCH3* expression in each tumor type.

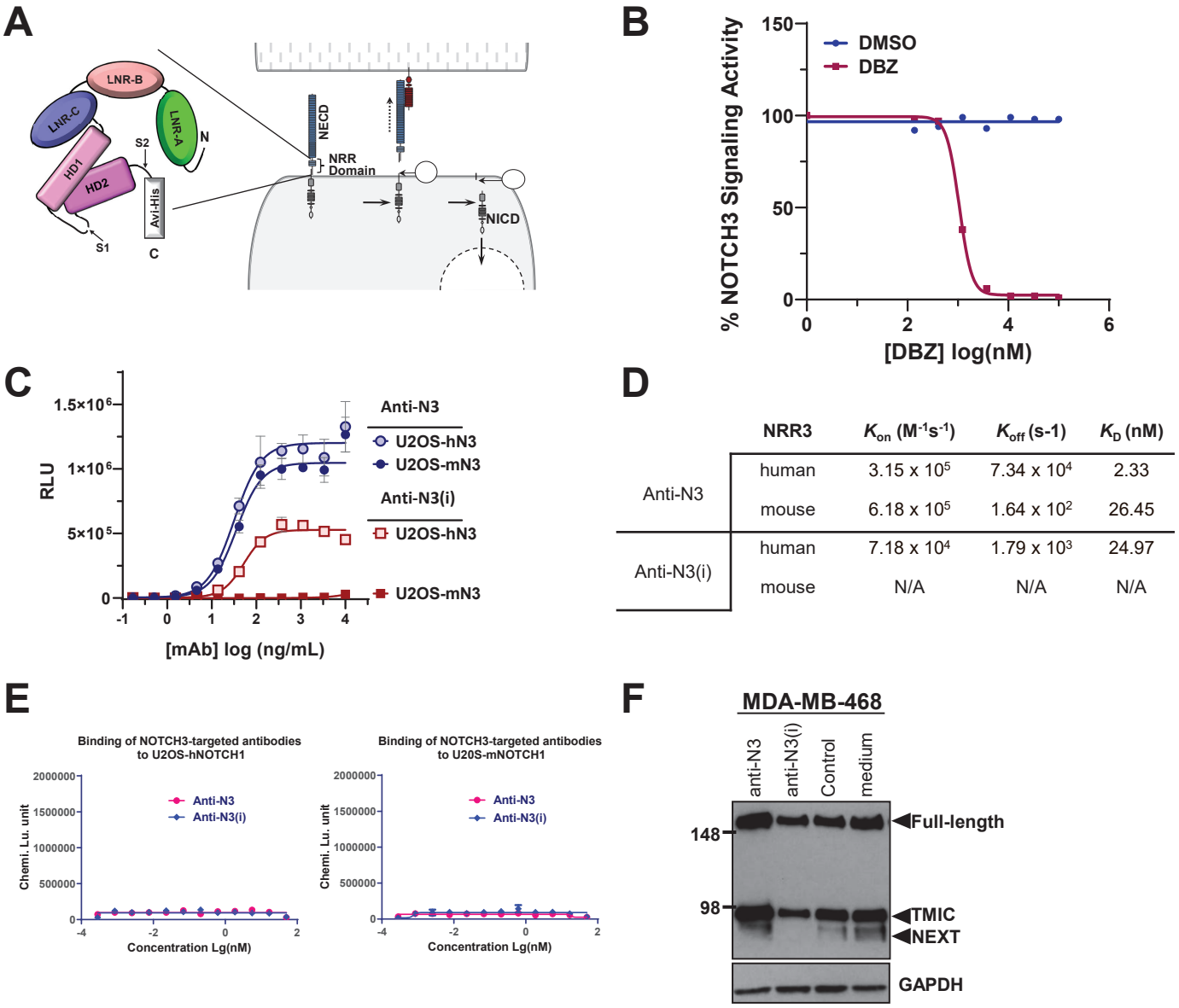

	NRR3	K_{on} ($M^{-1}s^{-1}$)	K_{off} (s-1)	K_D (nM)
Anti-N3	human	3.15 x 10^5	7.34 x 10^4	2.33
	mouse	6.18 x 10^5	1.64 x 10^2	26.45
Anti-N3(i)	human	7.18 x 10^4	1.79 x 10^3	24.97
	mouse	N/A	N/A	N/A

Figure S2. Generation and Characterization of Therapeutic Anti-NOTCH3 mAbs. Related to Figure 2.

(A) Schematic of recombinant NRR domain generated from human or mouse NOTCH3 that was used for immunization of rats in relation to the full-length NOTCH3 receptor expressed on the cell surface. Following ligand binding, the NOTCH3 receptor undergoes a series of proteolytic cleavage events within the NRR leading to nuclear translocation of the NICD in the receptor cell and transendocytosis and internalization of the NECD into the ligand-expressing cell. (B) NOTCH3-dependent report gene assay in U2OS-hN3 Luc-reporter cells with γ-secretase inhibitor DBZ and DMSO control. Data represents mean ± SD (n = 3). (C) Cell surface binding ELISAs in which NOTCH3-targeted mAbs were tested for their binding to U2OS cells overexpressing human NOTCH3 (U2OS-hN3) or mouse NOTCH3 (U2OS-mN3), RLU = relative luminescence units. Data represents mean ± SD of 3 biological replicates (n = 3 per replicate). (D) The kinetic constants of the interactions between human or mouse NOTCH3 NRR and NOTCH3-targeted mAbs were determined by surface plasmon resonance (Biacore® T100, Biacore Inc., Piscataway, NJ). K_{on}, association rate or on rate; K_{off}, dissociation rate or off rate; K_d, dissociation constant which is calculated as K_{off}/K_{on}. (E) Cell surface binding ELISAs in which NOTCH3-targeted mAbs were tested for their binding to U2OS cells overexpressing human NOTCH1 (U2OS-hNOTCH1) or mouse NOTCH1 (U2OS-mNOTCH1). Representative data represents mean (n = 2). (F) Immunoblot using a C-terminal domain antibody to detect basal NOTCH3 signaling from MDA-MB-468 breast cancer cells following treatment with anti-NOTCH3 or control mAbs. GAPDH is shown as a loading control.

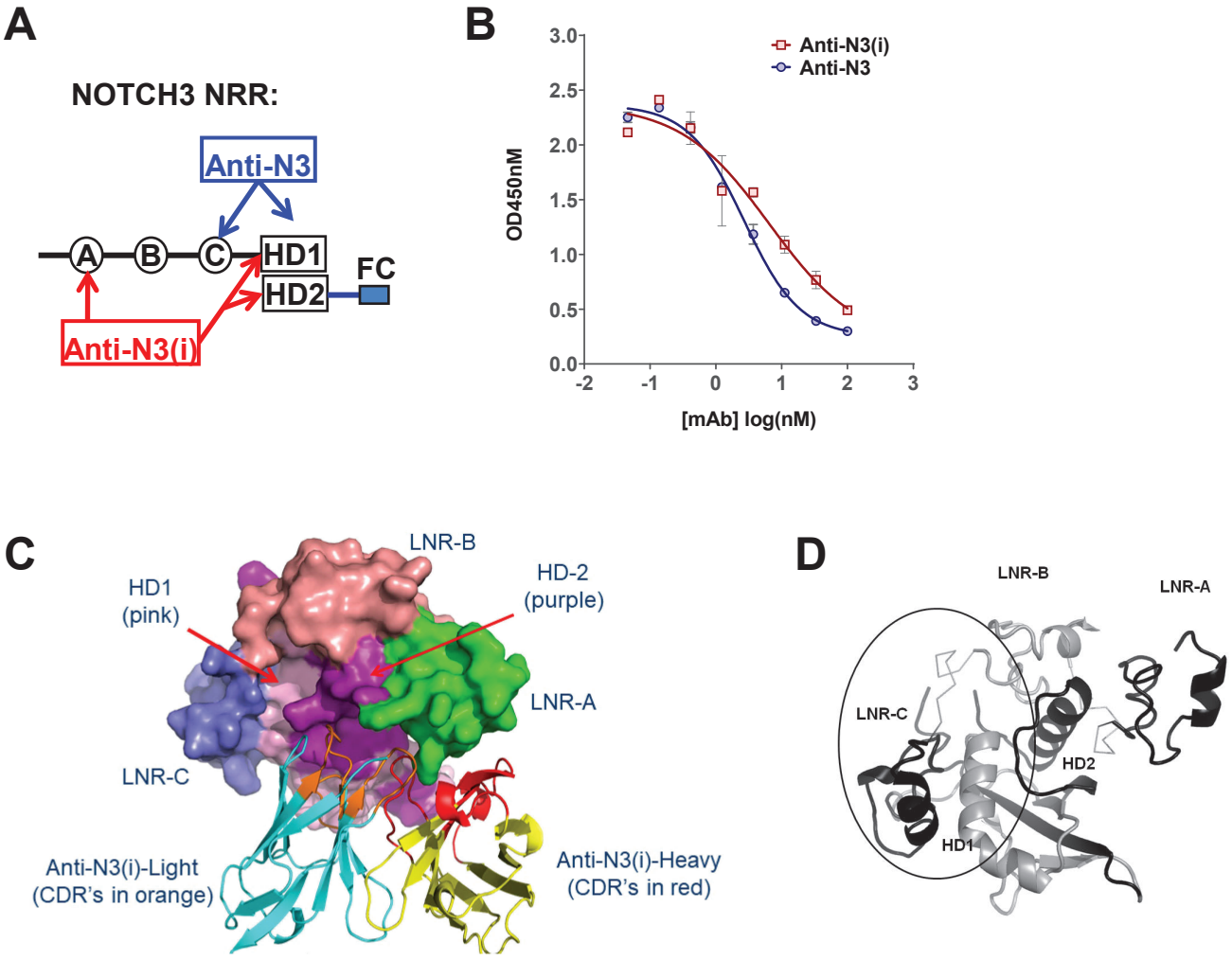

Figure S3. Generation and Characterization of Therapeutic Anti-NOTCH3 mAbs. Related to Figure 2.

(A) Diagram of heterodimeric NOTCH3 NRR that consists of the N-terminal polypeptide encompassing LNR-A, -B, -C and HD1 domains, and a C-terminal part containing HD2 domain fused with human IgG1 Fc fragment for ease of expression and purification. Two sub-domains are essential for anti-N3 binding to NOTCH3, the LNR-C and the HD1 domains. Three sub-domains are essential for anti-N3(i) binding to NOTCH3, the LNR-A, HD1 and HD2 domains. Components represented in the diagram are not proportional to their actual size. (B) Competition ELISA of NOTCH3-targeted mAbs with biotinylated anti-N3 on U2OS-hN3 cells. Representative data represents mean ± SEM (n =2). (C) Structure of anti-N3(i) variable domain bound to NOTCH3 NRR. The heavy (yellow) and light (cyan) chain variable domains of mAb clone 75 are shown as ribbons. The NOTCH3 NRR is shown as a Van der Waals surface colored by sub-domain as shown. Anti-N3(i) heavy chain CDRs (red) bind to the NOTCH3 NRR LNR-A and HD-2 subdomains while anti-N3(i) light chain CDRs (orange) binds to the HD-1 and HD-2 subdomains. (D) Crystal structure of the NOTCH3 NRR showing expected anti-N3 binding epitope. LNR-A, LNR-C, and HD1 are shown in black. LNR-B and HD2 are shown in gray. The linkers between the LNR regions are shown as thin ribbons. The large ellipse encloses the expected epitope for anti-N3, based on epitope mapping using NOTCH3-NOTCH1 chimeric constructs.

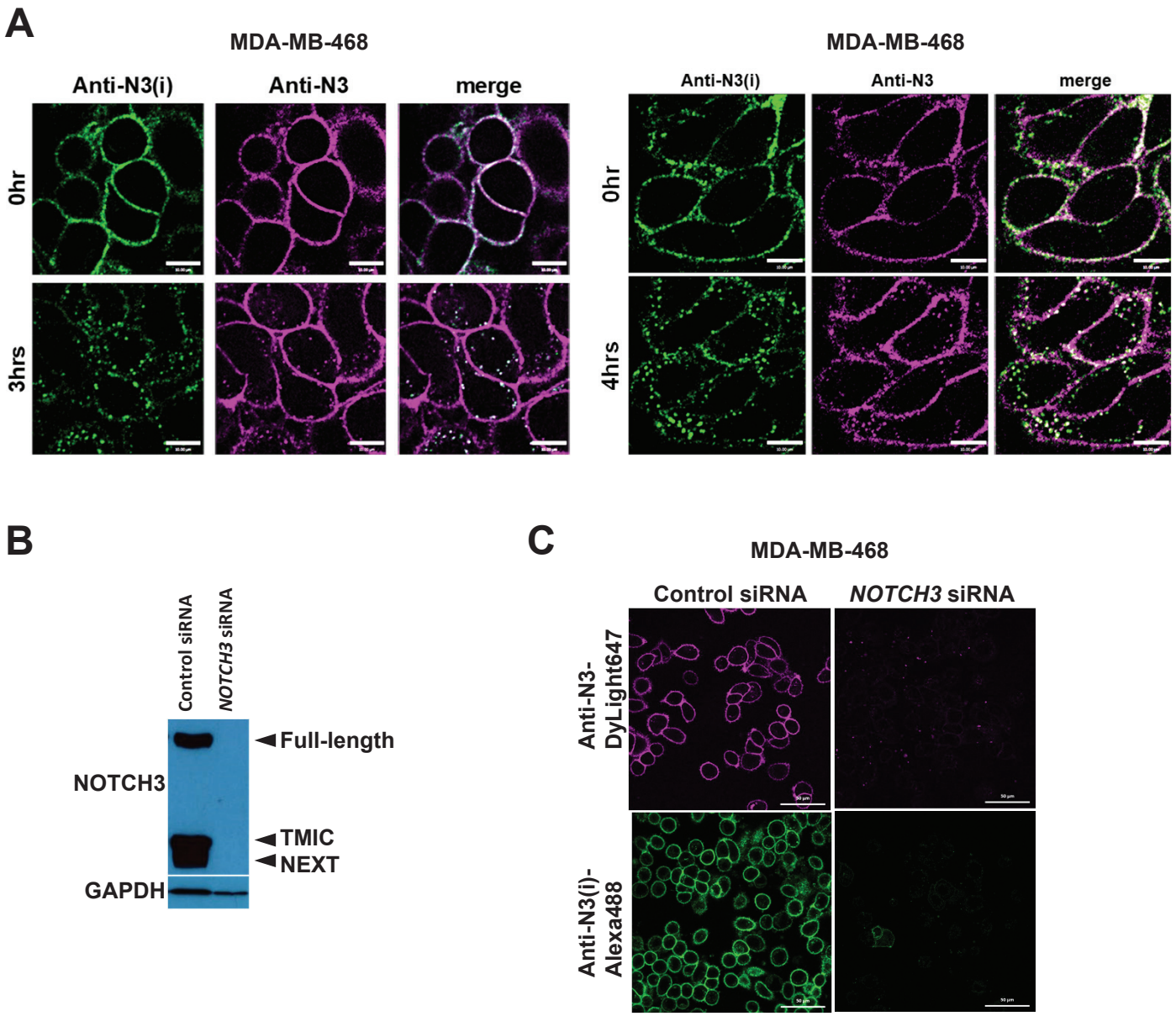

Figure S4. Cell Membrane Distribution of Anti-NOTCH3 mAbs Depends on Signaling Status. Related to Figure 3.

(A) Additional examples of single optical sections from live cell confocal imaging of NOTCH3-targeted mAbs simultaneously bound to MDA-MB-468 cells and imaged over time. Anti-N3(i)-Alexa 488 (green), anti-N3-DyLight647 (magenta), scale bar, 10 µm. (B) Immunoblot of NOTCH3 using a C-terminal domain antibody from MDA-MB-468 breast cancer cells following siRNA knockdown of *NOTCH3* expression. GAPDH is shown as a loading control. (C) Single optical sections from confocal imaging of NOTCH3-targeted mAbs bound to fixed MDA-MB-468 cells after siRNA knockdown of *NOTCH3* expression. Anti-N3(i)-Alexa647 (magenta), anti-N3-Alexa488 (green), scale bar, 50 µm.

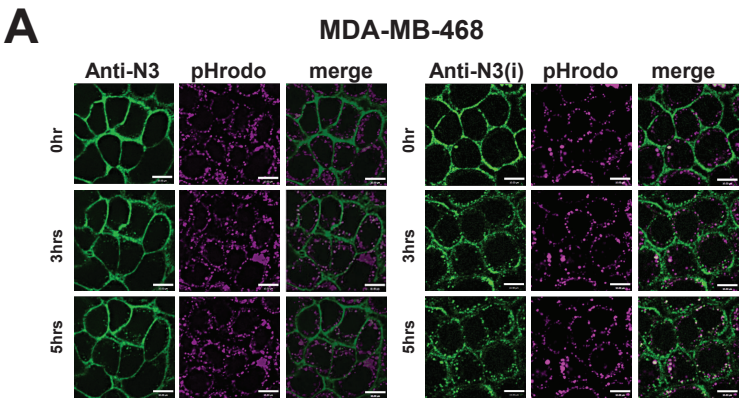

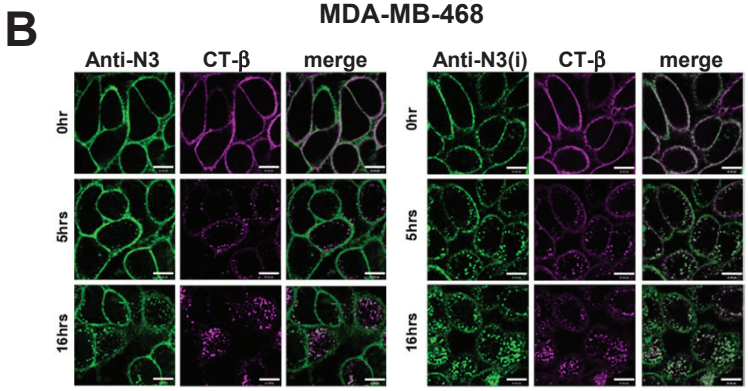

C

TIME (Hours)	0	3	8	24
CAV-1	ns	$p = 0.0346$	$p = 0.0004$	$p = 0.0160$
Clathrin	ns	ns	ns	ns

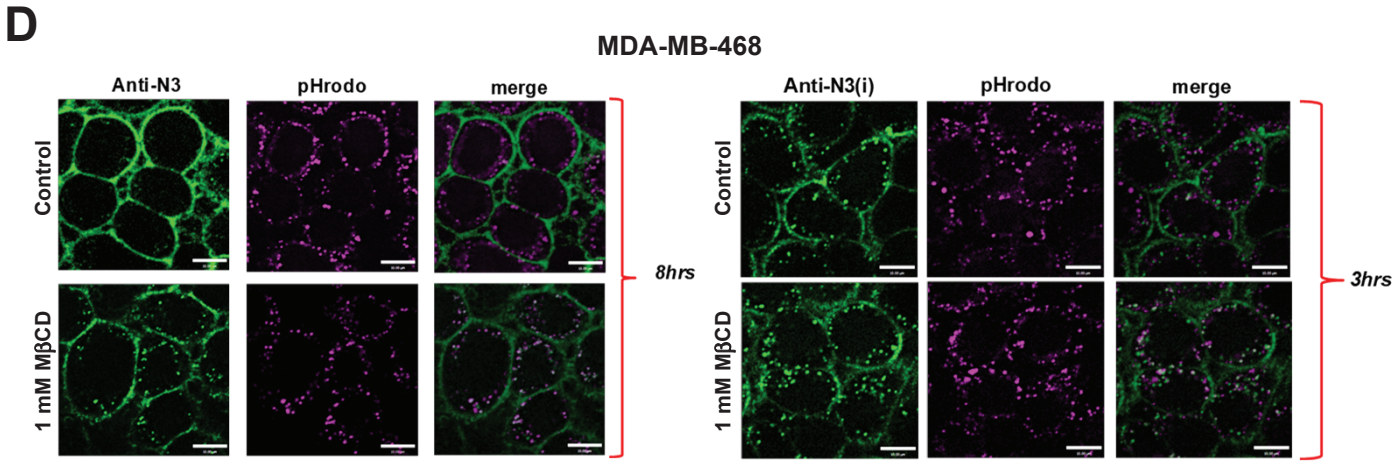

Figure S5. Anti-NOTCH3 mAbs have Differential Rates of Endocytosis and Lysosomal Trafficking. Related to Figure 4.

(A) Additional examples of single optical sections from live cell confocal imaging of NOTCH3-targeted mAbs colocalized with pHrodo red dextran in MDA-MB-468 cells over time and used to generate graphs in Figure 4A. (B) Additional example of single optical sections from live cell confocal imaging of NOTCH3-targeted mAbs colocalized with CT-β in MDA-MB-468 cells over time and used to generate graphs in Figure 4C. (C) Statistical analysis of MCC values generated from anti-N3 vs anti-N3(i) co-localization with anti-CAV1 or anti-clathrin antibodies using an unpaired t-test, ns, non-significant. (D) Additional example of single optical sections from live cell confocal imaging of NOTCH3-targeted mAbs colocalized with pHrodo-Red dextran in MβCD treated MDA-MB-468 cells over time and used to generate graphs in Figure 4F. Scale bar, 10 μm in all panels.

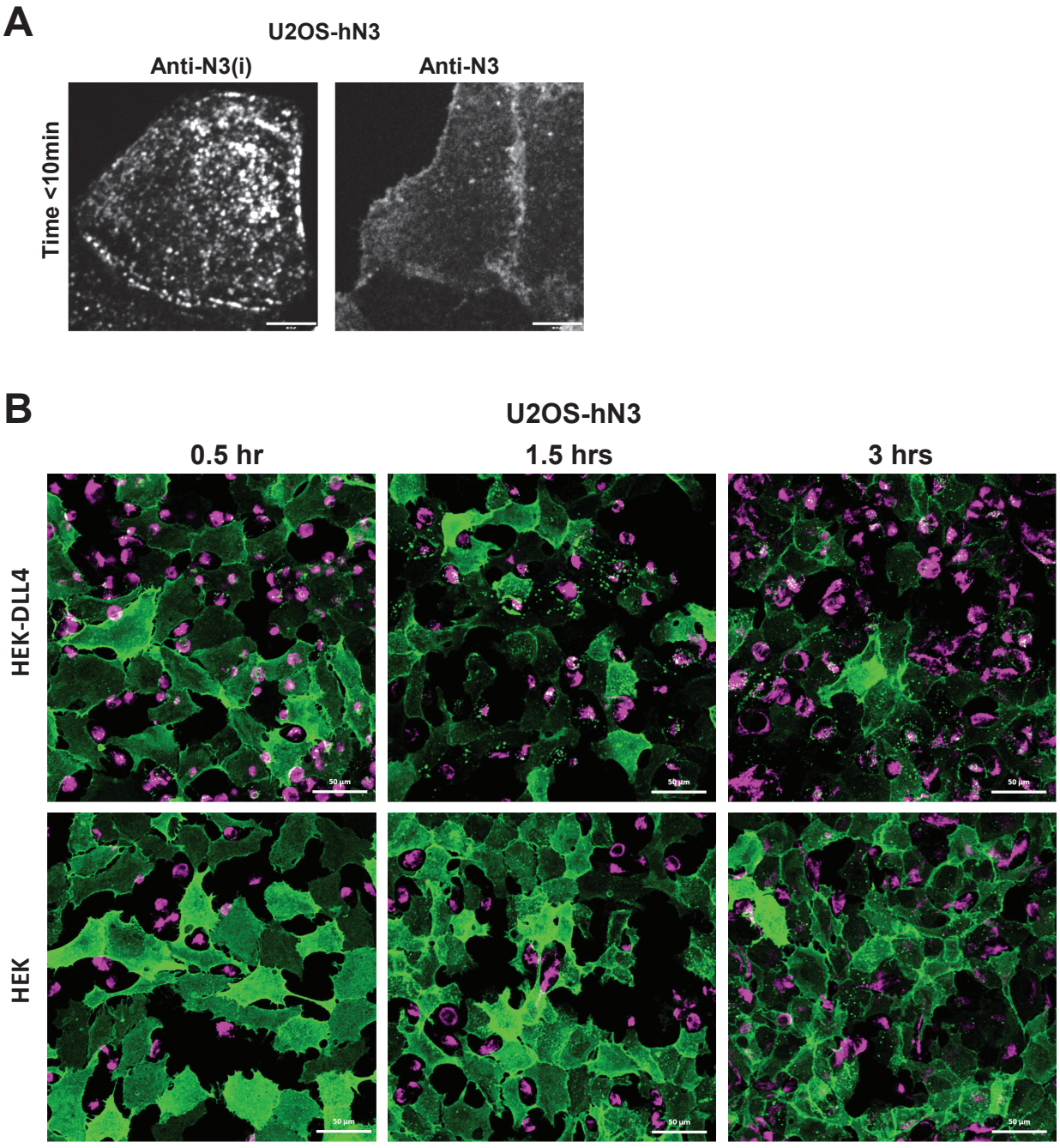

Figure S6. Anti-NOTCH3 mAbs Transendocytose into DLL4 Ligand-expressing Cells. Related to Figure 5.

(A) Maximum intensity projections from live cell confocal imaging of NOTCH3-targeted mAbs that were bound to U2OS-hN3 cells and then co-cultured with HEK-DLL4 cells. Images are examples of U2OS-hN3 cells that were not in contact with HEK-DLL4 cells. Scale bar, 10 µm. (B) Confocal images of U2OS-hN3 cells that were bound by the anti-N3 mAb and co-cultured with HEK-control or HEK-DLL4 cells (magenta) that were then fixed and stained at the indicated time points. The anti-N3 mAb was detected by indirect immunofluorescence (green). Scale bar = 50 µm.

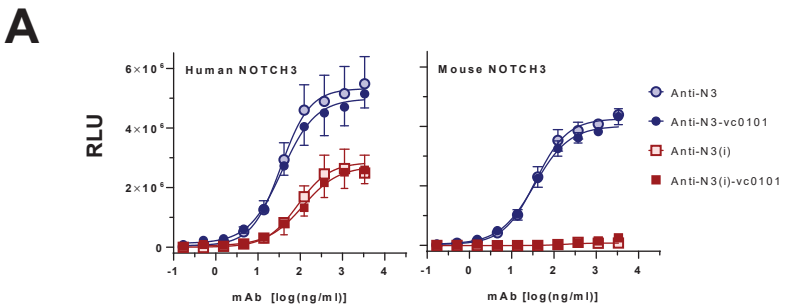

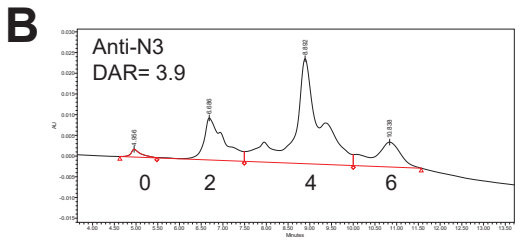

DAR	Retention Time	% Area
0	4.956	1.79
2	6.686	19.47
4	8.892	63.21
6	10.838	15.52

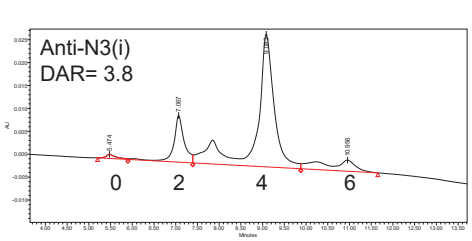

DAR	Retention Time	% Area
0	5.474	1.28
2	7.067	15
4	9.083	73
6	10.956	10.64

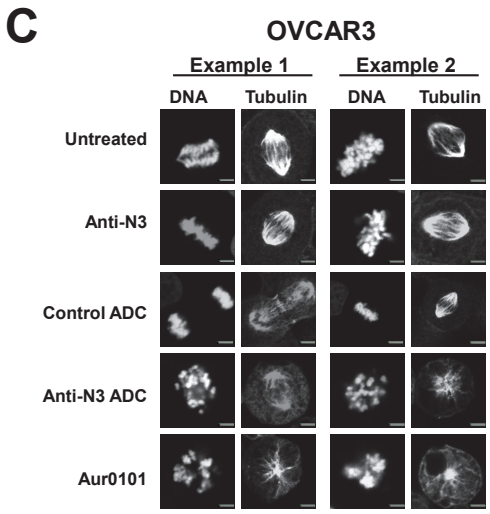

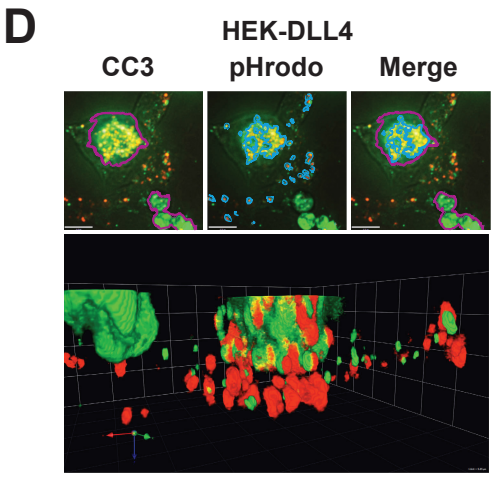

Figure S7. NOTCH3-targeted ADCs induce Cytotoxicity in Both Receptor and Ligand Cells. Related to Figure 6.

(A) Cell surface binding ELISAs in which NOTCH3-targeted mAbs were directly compared to NOTCH3-ADCs for their binding to U2OS cells overexpressing human NOTCH3 or mouse NOTCH3. Data represents mean ± SD from 3 biological replicates (n = 3 per replicate), RLU = relative luminescence units. (B) Drug-to-antibody ratios (DAR) and distributions for representative batches of NOTCH3-targeted ADCs as analyzed by hydrophobic interaction chromatograph. (C) OVCAR3 cells were treated for 48 hrs with 1 mg/mL of anti-N3 mAb, anti-N3 ADC, control ADC, and 0.1 nM free auristatin payload (PF-06380101). Cells were fixed, permeabilized and processed for immunofluorescence staining with anti-α-tubulin antibody and DAPI to stain DNA. Images were acquired with an 63X objective (2X magnification) on a Zeiss LSM510 laser scanning confocal microscope. Scale bar = 5 μm. (D) z stack of maximum intensity projections from live cell confocal imaging of anti-N3 ADC bound to U2OS-hN3 cells and co-cultured with HEK-DLL4 cells labeled with pHrodo Red dextran. Caspase compartments (magenta line), pHrodo Red dextran compartments (blue line) and the merged image.

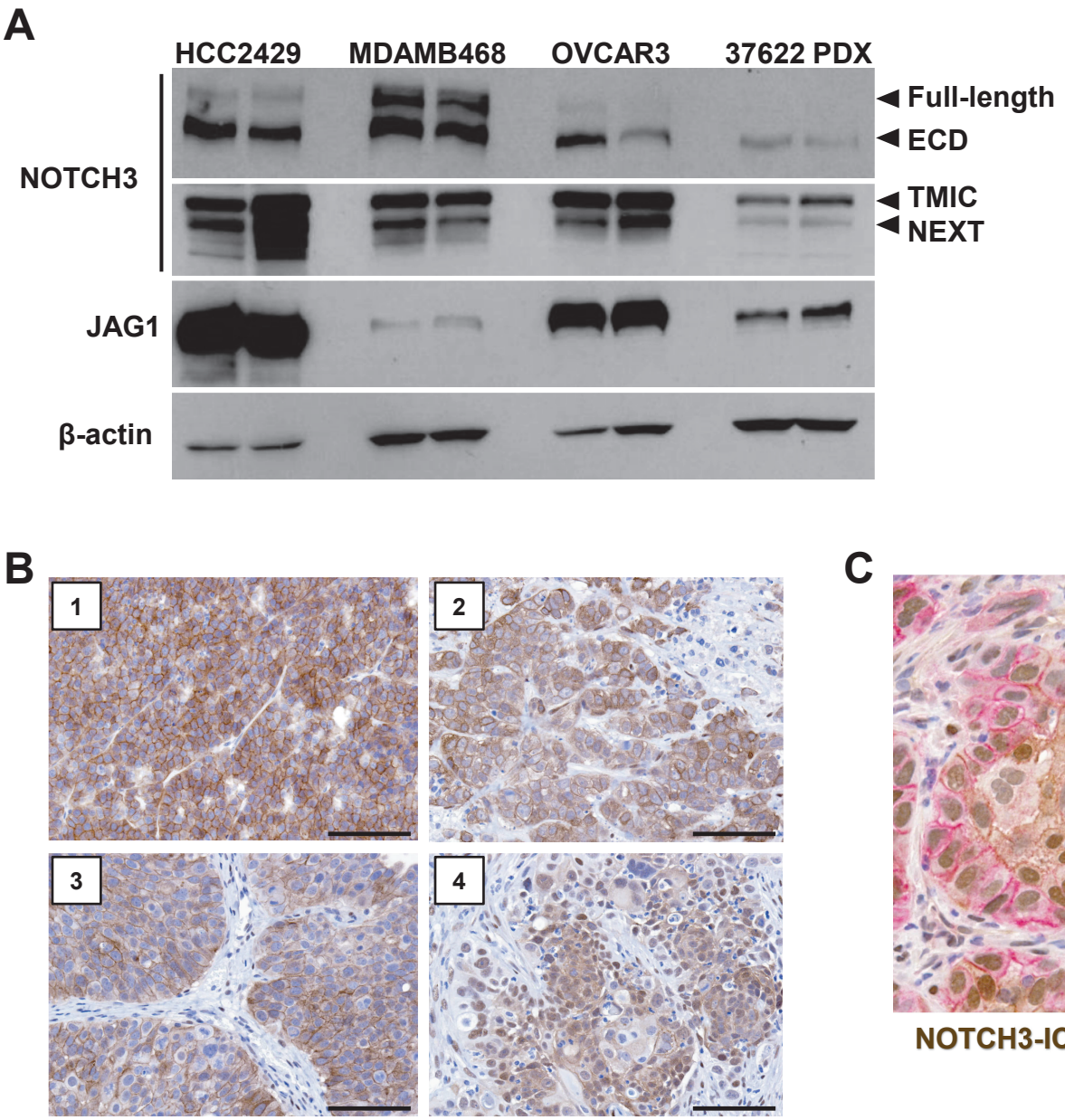

Figure S8. NOTCH3-targeted ADCs induce Prolonged Tumor Regressions. Related to Figure 7.

(A) Extracts from 2 individual tumor xenografts were immunoblotted with antibodies specific to the N-terminal NOTCH3 extracellular domain (NECD), the C-terminal NOTCH3 intracellular domains (TMIC/NEXT), JAG1 ligand and β-actin as a control. (B) Immunohistochemistry was performed on tumor xenografts using the C-terminal anti-NOTCH3 intracellular domain antibody that detected membrane-associated, cytoplasmic and nuclear NOTCH3 in (1) HCC2429 model; (2) MDA-MB-468 model; (3) OVCAR3 model; and (4) 37622 PDX model. Scale bar, 100 μm. (C) Immunohistochemistry was performed on the 37622 PDX model and co-stained brown with the C-terminal anti-NOTCH3 intracellular domain antibody that detected membrane-associated, cytoplasmic and nuclear NOTCH3 and magenta with an anti-JAG1 antibody. Scale bar, 50 μm.

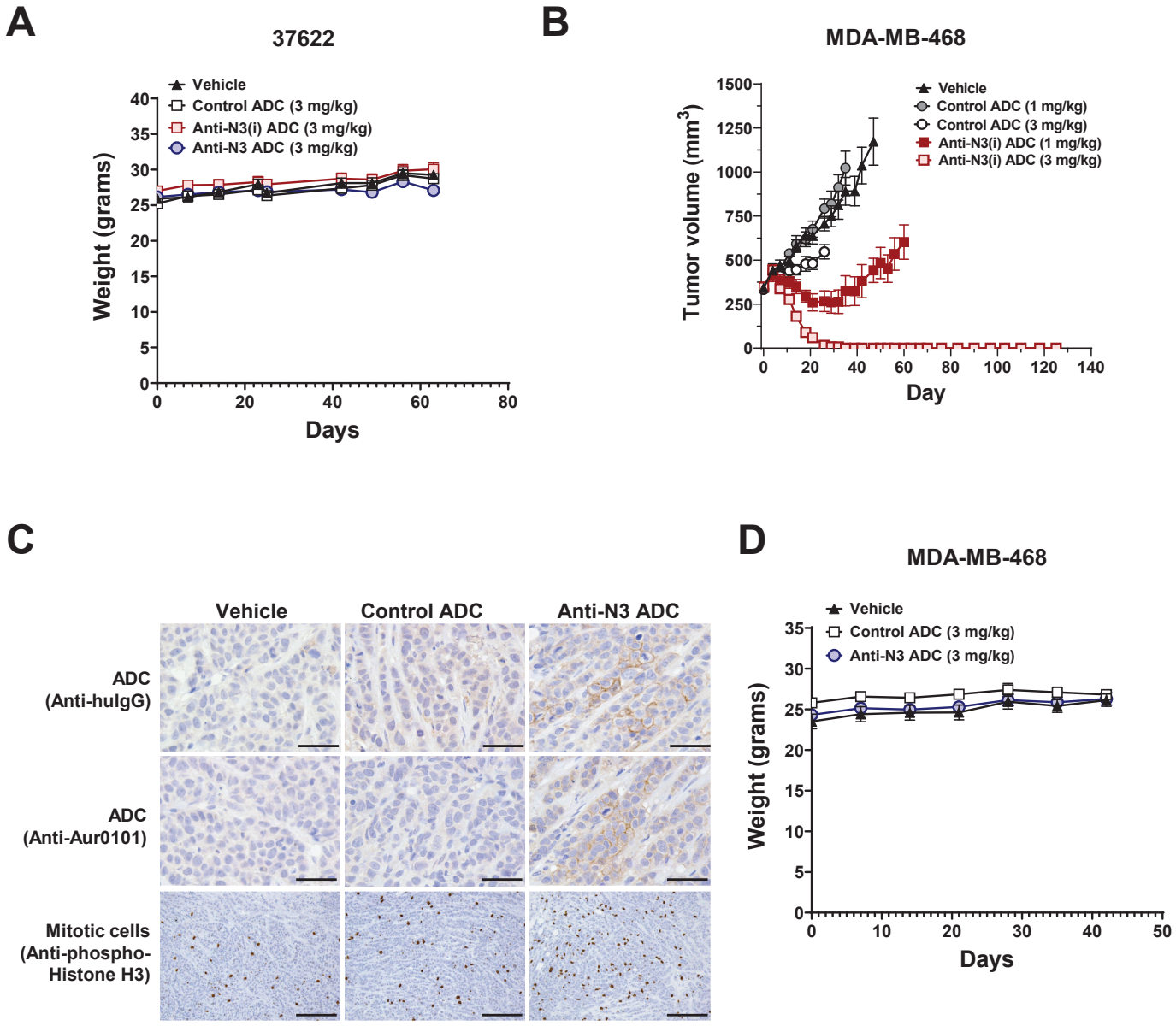

Figure S9. NOTCH3-targeted ADCs induce Prolonged Tumor Regressions. Related to Figure 7.

(A) Athymic nu/nu mouse body weights from NOTCH3-targeted or control ADC-treated 37622 PDX model dosed at 3 mg/kg every 4 days for 4 times starting at day 0. Data represent mean ± SEM (n = 9-10 per group). (B) Tumor growth inhibition of MDA-MB-468 CLX model treated with the anti-N3(i) ADC or control ADC dosed at 1 or 3 mg/kg every 4 days for 4 times starting at day 0. Data represent mean ± SEM (n = 7-8 per group). (C) Mice bearing MDA-MB-468 tumor xenografts were randomized into cohorts according to tumor volumes and dosed once intravenously with 3 mg/kg anti-N3 ADC, 3 mg/kg Control ADC or vehicle. After 24 hours, tumors were harvested, processed for immunohistochemistry and stained with anti-human IgG or anti-Aur0101 to detect the ADC, and anti-phospho-histone H3 to detect mitotic cells. Scale bar, 50 μm for IHC of ADC, and 200 μm for IHC of mitotic cells. (D) SHO mouse body weights from anti-N3 ADC or control ADC-treated MDA-MB-468 CLX model dosed at 3 mg/kg every 4 days for 4 times starting at day 0. Data represent mean ± SEM (n = 7-8 per group).

Table S1. Crystallographic Statistics. Related to Figure 2.

	Notch3/anti-N3(i) Fab Complex
Data collection	
Space Group	$P2_12_12_1$
Cell dimensions	
a, b, c (Å)	133.65Å 158.95Å 159.69Å
α, β, γ	90.00˚ 90.00˚ 90.00˚
Resolution (Å)	112.66 – 2.98
R_{merge} [b]	0.19 (1.099)
$I / \sigma I$	10.0 (1.7)
Completeness (%)	99.9 (100.0)
Redundancy	6.7 (6.7)
Refinement	
Resolution (Å)	112.66 – 2.98
No. reflections	70204 (3541)
R_{work} / R_{free} [c]	0.233/0.256
No. atoms	18917
Protein	18838
Ion	69
Solvent	10
Mean *B* Value	57.74
R.M.S. Deviations	
Bond lengths (Å)	0.008
Bond angles (°)	1.04

a Values in parentheses are for highest-resolution shell.
b Rmerge = $\Sigma|I - \langle I \rangle|/\Sigma I$, where *I* is observed intensity and is average intensity obtained from multiple observations of symmetry related reflections.
c Rwork = $\Sigma||Fo| - |Fc||/\Sigma|Fo|$, where F_o and F_c are observed and calculated structure factor amplitudes respectively. $R_{free} = R_{work}$, calculated using random reflections omitted from the refinement (number of reflections given in parentheses).